Electronic Research Archive

https://www.aimspress.com/journal/era

ERA, 34(9): 6905–6932.
DOI: 10.3934/era.2026300
Received: 09 June 2026
Revised: 20 July 2026
Accepted: 31 July 2026
Published: 12 August 2026

Research article

Dynamics of impulsive control in a predator–prey model with the fear effect and group defense

Longyang Song, Meng Zhang*, Xiaofei Ge, Xiaojing Wang, Songbai Guo and Jinlong Lv

School of Science, Beijing University of Civil Engineering and Architecture, Beijing 100044, China

* **Correspondence:** Email: zhangmeng@bucea.edu.cn.

Abstract: This paper investigates a predator–prey model incorporating both the fear effect and a Holling type IV functional response with group defense. In this model, the fear effect characterizes the suppression of prey reproduction caused by predator presence, whereas the Holling type IV functional response describes the enhanced group defense of prey at high densities. First, for the non-impulsive system, we analyze the positivity and boundedness of solutions, as well as the existence and local stability of equilibria. Second, when the equilibrium of the uncontrolled system fails to meet ecological management requirements, we introduce unilateral and bilateral state-feedback impulsive control strategies. The existence of order-one periodic solutions is established by the successor function method, and criteria for orbital asymptotic stability are derived using impulsive Floquet theory. Finally, numerical simulations validate the theoretical results, which provide a theoretical basis for designing ecologically balanced impulsive management strategies that suppress pest outbreaks while maintaining predator and prey populations within acceptable ranges.

Keywords: fear effect; group defense; Holling type IV functional response; state-feedback impulsive control; order-one periodic solutions; orbital asymptotic stability

1. Introduction

Predator–prey interactions are fundamental mechanisms that regulate population dynamics in ecological systems. Classical models mainly focus on the direct consumptive effects of predators on prey. However, extensive empirical evidence has shown that prey's perception of predation risk may also substantially affect prey behavior, physiology, and reproduction. This non-consumptive effect is generally referred to as the fear effect. For example, Zanette et al. reported that exposure to predator vocalizations alone reduced the annual offspring production of song sparrows by 40% [1–4]. From the perspective of mathematical modeling, the fear effect has been incorporated into single-species and predator–prey models to examine its impact on stability, bifurcation, and persistence [5–7].

In addition to the fear effect, group defense is another important mechanism that affects predation efficiency. When prey density increases, aggregation, vigilance, synchronized escape, and cooperative defense may reduce the capture success of predators. In aphid populations, collective defensive behaviors such as synchronous body shaking, twitching, and hind-leg kicking have been observed in response to attacks by natural enemies. Aphid alarm pheromones can also induce escape, dispersal, and defensive responses among conspecifics, thereby generating a group-level risk response [8,9]. The Holling type IV functional response can describe such nonmonotonic predation relationships and is commonly used to model the decline in predation efficiency caused by group defense [10–14]. Related extensions of predator–prey models have also examined habitat adaptation, spatial herd behavior, and nonlocal fear effects with delay [15–17]. Recently, the coupled effects of the fear effect and group defense have attracted increasing attention. Chen and Yang proposed a predator–prey model involving fear-induced group defense and a Monod–Haldane functional response [18]. Motivated by these studies, this paper further investigates the dynamical properties of this class of systems and the complex behaviors induced by impulsive control.

From a biological viewpoint, the model can be interpreted as the interaction between aphid pests and predatory natural enemies such as harlequin ladybirds. High densities of aphids may damage crops, whereas ladybirds can suppress aphid populations through predation [19]. Nevertheless, when the density of natural enemies is high and the target pest is scarce, these predators may attack non-target insects or compete with native natural enemies, thereby posing ecological risks [20]. Therefore, a reasonable management objective is not simply to eradicate pests but to prevent pest outbreaks while maintaining both pests and natural enemies within an ecologically acceptable range. Based on this idea, this paper analyzes the deterministic model and develops unilateral and bilateral state-feedback impulsive control strategies, with emphasis on the existence and stability of periodic solutions.

2. Deterministic model and preliminaries

2.1. Baseline model

Based on the above considerations, we formulate the following predator–prey model with the fear effect and group defense:

$$\begin{cases} \dfrac{dx}{dt} = \dfrac{rx}{1+ky}\left(1-\dfrac{x}{K}\right) - \dfrac{\beta xy}{1+ax+bx^2}, \\ \dfrac{dy}{dt} = \dfrac{c\beta xy}{1+ax+bx^2} - dy, \end{cases} \tag{2.1}$$

where $x = x(t)$ denotes the prey population density at time t and $y = y(t)$ denotes the predator population density at time t. System (2.1) is defined in the nonnegative quadrant $R^2_+ = \left\{(x,y) \in R^2 : x \geq 0, y \geq 0\right\}$. The biological interpretations of the parameters are as follows. The parameter r is the intrinsic growth rate of the prey; K is the environmental carrying capacity of the prey; k is the intensity coefficient for the fear effect; β is the predation rate; and a and b are group-defense parameters. Specifically, a reflects the defensive effect at low prey densities, whereas b represents the enhanced defense at high prey densities caused by collective defense, alarm pheromones, and group-level risk responses [8, 9]. The parameter c is the biomass conversion efficiency, which takes values between 0 and 1, and d is the natural mortality rate of the predator.

System (2.1) is not taken directly from a single existing model; rather, it is constructed by combining

several standard ecological mechanisms. The term $rx(1 - x/K)$ represents logistic prey growth, while the factor $1/(1 + ky)$ describes the reduction in prey reproduction caused by the fear of predators. The predation term $\beta xy/(1+ax+bx^2)$ is a Holling type IV functional response, which represents the decline in predation efficiency at high prey densities due to group defense. In the predator equation, c denotes the biomass conversion efficiency, and d denotes the natural mortality rate [6, 10, 12].

2.2. Preliminaries

To facilitate the analysis of state-feedback impulsive control systems, we briefly introduce the basic concepts of impulsive semi-dynamical systems and the criterion for orbital asymptotic stability [21–26]. Consider the following planar state-feedback impulsive semi-dynamical system:

$$\begin{cases} \frac{dx}{dt} = P(x, y), \ \frac{dy}{dt} = Q(x, y), & (x, y) \notin \mathcal{M}, \\ \Delta x = \alpha(x, y), \ \Delta y = \beta(x, y), & (x, y) \in \mathcal{M}, \end{cases}$$

where P, Q are continuously differentiable functions and $\mathcal{M}$ denotes the impulsive set. Moreover, $\Delta x = x^+ - x$ and $\Delta y = y^+ - y$ denote the instantaneous jumps at an impulse time, and (x^+, y^+) is the post-impulse point in the phase set $\mathcal{N}$.

Assume that the system admits an order-n periodic solution $\pi(t) = (\xi(t), \eta(t))$ with period T, which intersects the impulsive set exactly n times over one period. To determine its orbital asymptotic stability, we introduce the following impulsive Floquet criterion:

Lemma 2.1 (Impulsive Floquet multiplier criterion). If the multiplier μ satisfies $|\mu| < 1$, then the order-n periodic solution $\pi(t)$ is orbitally asymptotically stable, where

$$\mu = \prod_{j=1}^{n} \Delta_j \cdot \exp\left[\int_0^T \left(\frac{\partial P}{\partial \xi} + \frac{\partial Q}{\partial \eta}\right)|_{(\xi(t),\eta(t))} dt\right],$$

and the contribution factor Δ_j at each impulsive point is

$$\Delta_j = \frac{P_+\left(\frac{\partial B}{\partial \eta}\frac{\partial \phi}{\partial \xi} - \frac{\partial B}{\partial \xi}\frac{\partial \phi}{\partial \eta} + \frac{\partial \phi}{\partial \xi}\right) + Q_+\left(\frac{\partial A}{\partial \xi}\frac{\partial \phi}{\partial \eta} - \frac{\partial A}{\partial \eta}\frac{\partial \phi}{\partial \xi} + \frac{\partial \phi}{\partial \eta}\right)}{P\frac{\partial \phi}{\partial \xi} + Q\frac{\partial \phi}{\partial \eta}}|_{(\xi(t_j),\eta(t_j))},$$

where $(\xi(t_j), \eta(t_j))$ is the j-th impulsive point; $(\xi(t_j^+), \eta(t_j^+))$ is the corresponding post-impulse point; $P_+ = P(\xi(t_j^+), \eta(t_j^+))$, $Q_+ = Q(\xi(t_j^+), \eta(t_j^+))$; $A(x, y), B(x, y)$ are the impulsive mapping functions satisfying $\Delta x = A(x, y), \Delta y = B(x, y)$; $\phi(x, y) = 0$ defines the impulsive set $\mathcal{M}$; and all partial derivatives are evaluated at the impulsive point.

3. Dynamical analysis of the deterministic model

By the existence and uniqueness theorem for ordinary differential equations, the vector field of system (2.1) is continuously differentiable on R_+^2. Hence, for any initial condition $(x(0), y(0)) \in R_+^2$, system (2.1) admits a unique solution $(x(t), y(t))$ on a maximal interval of existence.

3.1. Positivity of solutions

Theorem 3.1. If $x(0) > 0$ and $y(0) > 0$, then the solution $(x(t), y(t))$ of system (2.1) satisfies $x(t) > 0$ and $y(t) > 0$ for all $t > 0$.

Proof. The two equations of system (2.1) can be rewritten in logarithmic derivative form as follows:

$$\frac{d}{dt}\ln x = \frac{r}{1+ky}\left(1-\frac{x}{K}\right) - \frac{\beta y}{1+ax+bx^2}, \tag{3.1}$$

$$\frac{d}{dt}\ln y = \frac{c\beta x}{1+ax+bx^2} - d. \tag{3.2}$$

Integrating (3.1) and (3.2) from 0 to t gives

$$x(t) = x(0)\exp\left\{\int_0^t \left[\frac{r}{1+ky(s)}\left(1-\frac{x(s)}{K}\right) - \frac{\beta y(s)}{1+ax(s)+bx(s)^2}\right]ds\right\}, \tag{3.3}$$

$$y(t) = y(0)\exp\left\{\int_0^t \left[\frac{c\beta x(s)}{1+ax(s)+bx(s)^2} - d\right]ds\right\}. \tag{3.4}$$

Since the exponential function is strictly positive and the initial values are positive, it follows that $x(t) > 0$ and $y(t) > 0$ for all t in the interval of existence. □

3.2. Boundedness of solutions

Theorem 3.2. All positive solutions of system (2.1) are ultimately uniformly bounded. More precisely,

$$\limsup_{t\to\infty} x(t) \le K, \qquad \limsup_{t\to\infty} y(t) \le cK + \frac{crK}{4d}.$$

Proof. Denote the right-hand side of the prey equation by $F(x, y)$. When $x > K$, both terms in $F(x, y)$ are non-positive, and the first term is strictly negative. Hence, a solution cannot cross the line $x = K$ from left to right, and

$$x(t) \le M_0 := \max\{x(0), K\}.$$

Moreover, for any $\varepsilon > 0$, $F(x, y)$ is strictly negative for $K + \varepsilon \le x \le M_0$ and $y \ge 0$. Since $F(x, y)$ tends to $-\infty$ as y tends to infinity uniformly for $x \in [K + \varepsilon, M_0]$, there exists $m(\varepsilon) > 0$ such that $F(x, y) \le -m(\varepsilon)$ on this region. Therefore, every solution enters the region $x \le K + \varepsilon$ in finite time. Consequently,

$$\limsup_{t\to\infty} x(t) \le K.$$

Define the auxiliary function

$$V(t) = x(t) + \frac{y(t)}{c}.$$

Along the solutions of system (2.1),

$$\frac{dV}{dt} = \frac{rx}{1+ky}\left(1-\frac{x}{K}\right) - \frac{d}{c}y.$$

For all $x \ge 0$ and $y \ge 0$,

$$\frac{rx}{1+ky}\left(1-\frac{x}{K}\right) \le \frac{rK}{4}.$$

Indeed, when $0 \le x \le K$, this follows from $1/(1+ky) \le 1$ and $x(1-x/K) \le K/4$; when $x > K$, the left-hand side is negative. Thus, for sufficiently large t such that $x(t) \le K + \varepsilon$,

$$\frac{dV}{dt} \le \frac{rK}{4} - \frac{d}{c}y = \frac{rK}{4} - d(V-x) \le \frac{rK}{4} + d(K+\varepsilon) - dV.$$

By the comparison theorem,

$$\limsup_{t\to\infty} V(t) \le K + \varepsilon + \frac{rK}{4d}.$$

Letting ε tend to zero gives

$$\limsup_{t\to\infty} V(t) \le K + \frac{rK}{4d}.$$

Since $0 \le x(t) \le V(t)$ and $0 \le y(t) \le cV(t)$, we obtain

$$\limsup_{t\to\infty} x(t) \le K, \qquad \limsup_{t\to\infty} y(t) \le cK + \frac{crK}{4d}.$$

Therefore, all positive solutions of system (2.1) are ultimately uniformly bounded. □

3.3. Existence and number of equilibria

The equilibria of system (2.1) satisfy

$$\begin{cases} \dfrac{rx}{1+ky}\left(1 - \dfrac{x}{K}\right) = \dfrac{\beta xy}{1+ax+bx^2}, \\ \dfrac{c\beta xy}{1+ax+bx^2} = dy. \end{cases} \tag{3.5}$$

Theorem 3.3.1. For any set of parameter values, system (2.1) always has two boundary equilibria:

$$E_0 = (0,0),\ E_K = (K,0).$$

Proof. Setting $y = 0$ in (3.5), we find that the second equation is automatically satisfied, whereas the first equation becomes $rx\left(1 - \frac{x}{K}\right) = 0$, which gives $x = 0$ or $x = K$. Hence, E_0 and E_K are always equilibria. □

Next, we consider a positive equilibrium $E^* = (x^*, y^*)$ with $x^* > 0$ and $y^* > 0$. Since $y > 0$, the second equation of (3.5) yields the quadratic equation

$$dbx^2 + (da - c\beta)x + d = 0. \tag{3.6}$$

Its discriminant is $\Delta = (da - c\beta)^2 - 4d^2b$. Equation (3.6) has real roots if and only if $\Delta \ge 0$, that is,

$$\beta \ge \frac{d\left(a + 2\sqrt{b}\right)}{c} \triangleq \beta_2. \tag{3.7}$$

By Vieta's formula, the product of the two roots is $\frac{1}{b} > 0$, and their sum is $\frac{c\beta - da}{db}$. Hence, both roots are positive if $c\beta - da > 0$, i.e.,

$$\beta > \frac{da}{c} \triangleq \beta_1. \tag{3.8}$$

Since $\beta_2 > \beta_1$, the condition $\beta > \beta_1$ is automatically satisfied when $\beta \geq \beta_2$. Therefore, the condition for the existence of positive roots is $\beta \geq \beta_2$. Assume that $\beta \geq \beta_2$. Then the two roots of (3.6) are

$$x_1 = \frac{c\beta - da - \sqrt{(c\beta - da)^2 - 4d^2b}}{2db}, \quad x_2 = \frac{c\beta - da + \sqrt{(c\beta - da)^2 - 4d^2b}}{2db}. \tag{3.9}$$

By Vieta's formula $x_1 x_2 = \frac{1}{b}$,

$$0 < x_1 \leq \frac{1}{\sqrt{b}} \leq x_2,$$

where equality holds if and only if $\beta = \beta_2$. For each positive root x_i $(i = 1, 2)$, the corresponding value of y can be obtained from the first equation of (3.5). Let $P_i = 1 + ax_i + bx_i^2$. Then

$$\beta k y^2 + \beta y - rP_i\left(1 - \frac{x_i}{K}\right) = 0. \tag{3.10}$$

If $x_i < K$, then (3.10) has a unique positive root

$$y_i^* = \frac{-\beta + \sqrt{\beta^2 + 4\beta k r P_i\left(1 - \frac{x_i}{K}\right)}}{2\beta k}. \tag{3.11}$$

If $x_i \geq K$, then (3.10) has no nonnegative real root, and hence such a root x_i does not yield a feasible positive equilibrium. Thus, depending on the relationship between β and β_2 and on the positions of x_1, x_2 relative to K, positive equilibria occur only in the following cases.

Theorem 3.3.2. If $\beta = \beta_2$ and $\frac{1}{\sqrt{b}} < K$, then system (2.1) has a unique positive equilibrium $E^* = (x^*, y^*)$, where $x^* = \frac{1}{\sqrt{b}}$, $y^* = \frac{-\beta_2 + \sqrt{\beta_2^2 + 4\beta_2 k r P\left(1 - \frac{1}{\sqrt{b}K}\right)}}{2\beta_2 k}$, and $P = 2 + \frac{a}{\sqrt{b}}$.

Proof. When $\beta = \beta_2$, we have $\Delta = 0$, and (3.6) has the double root $x^* = \frac{1}{\sqrt{b}}$. Since $x^* < K$, substituting it into (3.10) yields a positive root y^*. Hence, $E^* = (x^*, y^*)$ is the unique positive equilibrium. □

Theorem 3.3.3. If $\beta > \beta_2$ and the two roots of (3.6) satisfy $x_1 < K \leq x_2$, then system (2.1) has a unique positive equilibrium $E_1^* = \left(x_1, y_1^*\right)$, where x_1 is given by the first expression in (3.9) and y_1^* is obtained from (3.11) by taking $i = 1$.

Proof. When $\beta > \beta_2$, (3.6) has two distinct positive roots $x_1 < x_2$, with $x_1 < \frac{1}{\sqrt{b}} < x_2$. The condition $x_1 < K \leq x_2$ ensures that only x_1 satisfies $x < K$. Therefore, (3.10) gives a unique positive root y_1^*, and $E_1^* = \left(x_1, y_1^*\right)$ is the unique positive equilibrium. □

Theorem 3.3.4. If $\beta > \beta_2$ and the two roots of (3.6) satisfy $x_1 < x_2 < K$, then system (2.1) has two positive equilibria $E_1^* = \left(x_1, y_1^*\right)$ and $E_2^* = \left(x_2, y_2^*\right)$, where x_1, x_2 are given by (3.9) and y_i^*, $i = 1, 2$ are obtained from (3.11).

Proof. When $\beta > \beta_2$, (3.6) has two distinct positive roots $x_1 < x_2$, with $x_1 < \frac{1}{\sqrt{b}} < x_2$. The condition $x_2 < K$ implies that both roots satisfy $x_i < K$. Thus, substituting them into (3.10) yields two positive roots y_1^*, y_2^*, and the system has two positive equilibria. □

3.4. Stability analysis

Let

$$f(x,y)=\frac{rx}{1+ky}\left(1-\frac{x}{K}\right)-\frac{\beta xy}{1+ax+bx^2},\ g(x,y)=\frac{c\beta xy}{1+ax+bx^2}-dy.$$

Then the Jacobian matrix of system (2.1) is

$$J(x,y)=\begin{pmatrix}\frac{\partial f}{\partial x} & \frac{\partial f}{\partial y}\\ \frac{\partial g}{\partial x} & \frac{\partial g}{\partial y}\end{pmatrix},$$

where

$$\begin{aligned}\frac{\partial f}{\partial x}&=\frac{r\left(1-\frac{2x}{K}\right)}{1+ky}-\frac{\beta y\left(1-bx^2\right)}{(1+ax+bx^2)^2},\\ \frac{\partial f}{\partial y}&=-\frac{rxk\left(1-\frac{x}{K}\right)}{(1+ky)^2}-\frac{\beta x}{1+ax+bx^2},\\ \frac{\partial g}{\partial x}&=\frac{c\beta y\left(1-bx^2\right)}{(1+ax+bx^2)^2},\\ \frac{\partial g}{\partial y}&=\frac{c\beta x}{1+ax+bx^2}-d.\end{aligned}$$

Theorem 3.4.1. For the two boundary equilibria $E_0=(0,0)$ and $E_K=(K,0)$ of system (2.1), the following conclusions hold:
(i) E_0 is always a saddle point.
(ii) E_K is locally asymptotically stable if and only if $\frac{c\beta K}{1+aK+bK^2}<d$. If $\frac{c\beta K}{1+aK+bK^2}>d$, then E_K is a saddle point.

Proof. A direct computation gives

$$J(0,0)=\begin{pmatrix}r & 0\\ 0 & -d\end{pmatrix},$$

whose eigenvalues are $\lambda_1=r>0$ and $\lambda_2=-d<0$. Hence, E_0 is a saddle point. At E_K,

$$J(K,0)=\begin{pmatrix}-r & -\frac{\beta K}{1+aK+bK^2}\\ 0 & \frac{c\beta K}{1+aK+bK^2}-d\end{pmatrix},$$

with eigenvalues $\lambda_1=-r<0$ and $\lambda_2=\frac{c\beta K}{1+aK+bK^2}-d$. Therefore, E_K is a stable node if $\lambda_2<0$ and is a saddle point if $\lambda_2>0$. □

Next, we analyze the stability of the positive equilibria. Let $E^*=(x^*,y^*)$ be any positive equilibrium of system (2.1). Then it satisfies

$$\frac{c\beta x^*}{1+ax^*+bx^{*2}}=d, \tag{3.12}$$

$$\frac{rx^*}{1+ky^*}\left(1-\frac{x^*}{K}\right)=\frac{\beta x^*y^*}{1+ax^*+bx^{*2}}. \tag{3.13}$$

From (3.12), $\frac{\partial g}{\partial y}=0$ at E^*, and hence

$$J(E^*)=\begin{pmatrix}a_{11} & a_{12}\\ a_{21} & 0\end{pmatrix},$$

where

$$a_{11} = \frac{r\left(1 - \frac{2x^*}{K}\right)}{1 + ky^*} - \frac{\beta y^*\left(1 - bx^{*2}\right)}{P^2},$$
$$a_{12} = -\frac{rx^*k\left(1 - \frac{x^*}{K}\right)}{(1 + ky^*)^2} - \frac{\beta x^*}{P},$$
$$a_{21} = \frac{c\beta y^*\left(1 - bx^{*2}\right)}{P^2}.$$

Here, $P = 1 + ax^* + bx^{*2}$. The characteristic equation is

$$\lambda^2 - a_{11}\lambda - a_{12}a_{21} = 0. \tag{3.14}$$

Since $a_{12} < 0$, the sign of $\det(J) = -a_{12}a_{21}$ is the same as that of a_{21}. If $a_{21} < 0$, then $\det(J) < 0$, and E^* is a saddle point. If $a_{21} > 0$, then $\det(J) > 0$, and the sign of the real parts of the eigenvalues is determined by a_{11}. The sign of a_{21} is completely determined by $1 - bx^{*2}$.

Theorem 3.4.2. If $\beta = \beta_2$ and $\frac{1}{\sqrt{b}} < K$, then system (2.1) has a unique positive equilibrium $E^* = (x^*, y^*)$ with $x^* = \frac{1}{\sqrt{b}}$. In this case, E^* is non-hyperbolic.

Proof. By Theorem 3.3.2, $x^* = \frac{1}{\sqrt{b}}$. Hence, $1 - bx^{*2} = 0$. Substituting this into a_{21} gives $a_{21} = 0$. Therefore, $\det(J) = 0$, and the Jacobian matrix has at least one zero eigenvalue. Thus, the equilibrium is non-hyperbolic. □

Theorem 3.4.3. If $\beta > \beta_2$ and $x_1 < K \leq x_2$, then system (2.1) has a unique positive equilibrium $E_1^* = \left(x_1, y_1^*\right)$, where x_1 is given by the first expression in (3.9) and y_1^* is obtained from (3.11) by taking $i = 1$. If $K < \frac{1+2ax_1+3bx_1^2}{a+2bx_1}$, then E_1^* is locally asymptotically stable and is either a stable node or a stable focus; if $K > \frac{1+2ax_1+3bx_1^2}{a+2bx_1}$, then E_1^* is either an unstable node or an unstable focus; if $K = \frac{1+2ax_1+3bx_1^2}{a+2bx_1}$, then E_1^* is non-hyperbolic, and a Hopf bifurcation may occur.

Proof. Since $x_1 < \frac{1}{\sqrt{b}}$, we have $1 - bx_1^2 > 0$, and hence $a_{21} > 0$ and $\det(J) > 0$. The stability of E_1^* is therefore determined by the sign of

$$a_{11} = \frac{r}{1 + ky_1^*}\left[\left(1 - \frac{2x_1}{K}\right) - \frac{\left(1 - bx_1^2\right)\left(1 - \frac{x_1}{K}\right)}{P_1}\right],$$

where $P_1 = 1 + ax_1 + bx_1^2$. From (3.13),

$$\frac{\beta y_1^*}{P_1} = \frac{r}{1 + ky_1^*}\left(1 - \frac{x_1}{K}\right).$$

Substitution and simplification yield

$$a_{11} = \frac{r}{1 + ky_1^*} \cdot \frac{x_1}{P_1}\left[a + 2bx_1 - \frac{1 + 2ax_1 + 3bx_1^2}{K}\right].$$

Since $\frac{r}{1+ky_1^*} > 0$ and $\frac{x_1}{P_1} > 0$, the sign of a_{11} is determined by the bracketed term. Thus, E_1^* is locally asymptotically stable when $K < \frac{1+2ax_1+3bx_1^2}{a+2bx_1}$, unstable when $K > \frac{1+2ax_1+3bx_1^2}{a+2bx_1}$, and non-hyperbolic when equality holds. □

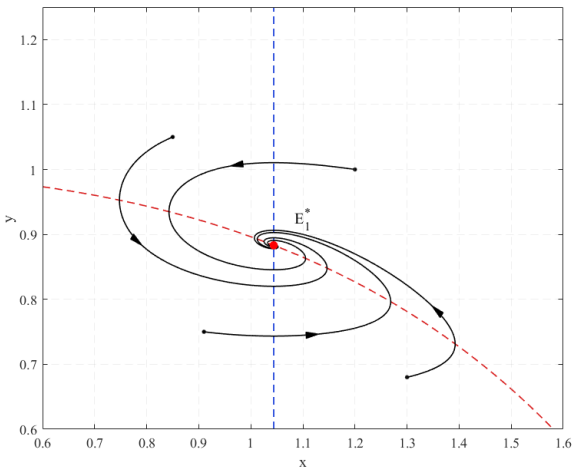

Figure 1. Phase portrait of the deterministic system showing a unique positive equilibrium that is a stable focus. Parameter values: $r = 2$, $K = 2$, $k = 1$, $\beta = 1$, $a = 0.5$, $b = 0.2$, $c = 0.5$, $d = 0.3$.

Theorem 3.4.4. If $\beta > \beta_2$ and $x_2 < K$, then system (2.1) has two positive equilibria $E_1^* = \left(x_1, y_1^*\right)$ and $E_2^* = \left(x_2, y_2^*\right)$, where x_1, x_2 are given by (3.9) and y_i^* by (3.11). Their stability properties are as follows:
(i) E_2^* is always a saddle point.
(ii) The stability condition of E_1^* is the same as that given in Theorem 3.4.3.

Proof. Since $x_1 x_2 = \frac{1}{b}$, we have $x_1 < \frac{1}{\sqrt{b}} < x_2$. Thus, $1 - bx_1^2 > 0$ and $1 - bx_2^2 < 0$. At E_2^*, $a_{21}^{(2)} < 0$, and hence $\det(J) < 0$ and the eigenvalues have opposite signs. Therefore, E_2^* is a saddle point. At E_1^*, $a_{21}^{(1)} > 0$ and $\det(J) > 0$, and its stability is determined by the trace. The derivation is identical to that in Theorem 3.4.3. □

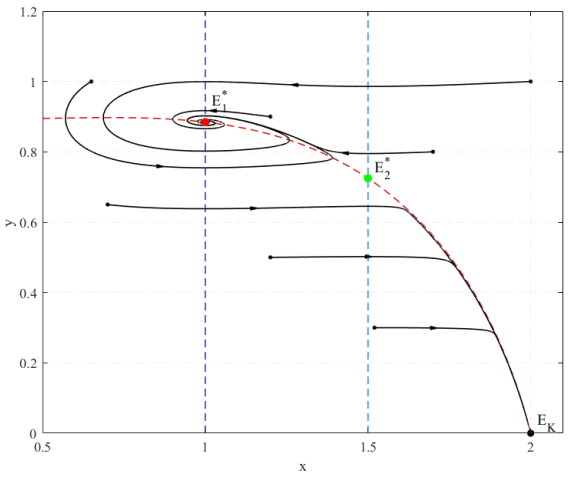

Figure 2. Phase portrait of the deterministic system with two positive equilibria, where the smaller equilibrium is stable and the larger one is a saddle point. Parameter values: $r = 2$, $K = 2$, $k = 1$, $\beta = 1.12$, $a = 0.2$, $b = 2/3$, $c = 0.5$, $d = 0.3$.

The existence and stability of equilibria are summarized in Table 1.

Table 1. Summary of equilibria and their stability.

Equilibrium	Existence condition	Type	Stability condition
$E_0 = (0, 0)$	Always exists	Saddle point	
$E_K = (K, 0)$	Always exists	Stable node	$\frac{c\beta K}{1+aK+bK^2} < d$
		Saddle point	$\frac{c\beta K}{1+aK+bK^2} > d$
E^* (double-root case)	$\beta = \beta_2,\ \frac{1}{\sqrt{b}} < K$	Non-hyperbolic	
E_1^* (single-root case)	$\beta > \beta_2,\ x_1 < K \le x_2$	Stable node/focus	$K < \frac{1+2ax_1+3bx_1^2}{a+2bx_1}$
		Unstable focus/node	$K > \frac{1+2ax_1+3bx_1^2}{a+2bx_1}$
		Non-hyperbolic	$K = \frac{1+2ax_1+3bx_1^2}{a+2bx_1}$
E_1^* (two equilibria)	$\beta > \beta_2,\ x_2 < K$	Same as above	Same as above
E_2^* (two equilibria)	$\beta > \beta_2,\ x_2 < K$	Saddle point	

4. Complex dynamics analysis under unilateral impulsive control

For system (2.1), if $\beta > \beta_2,\ x_1 < K \le x_2$, and $K < \frac{1+2ax_1+3bx_1^2}{a+2bx_1}$, then the system has a unique locally asymptotically stable positive equilibrium $E_1^* = (x_1, y_1^*)$. When the natural stable equilibrium cannot meet management requirements, a unilateral state-feedback impulsive control strategy is implemented once the prey density reaches the threshold A. In the aphid–ladybird system, this strategy represents artificial intervention when aphids approach the economic injury level, together with the release of ladybirds [19, 21, 22].

We formulate the following predator–prey model with state-feedback impulses:

$$\begin{cases} \dfrac{dx}{dt} = \dfrac{rx}{1+ky}\left(1-\dfrac{x}{K}\right) - \dfrac{\beta xy}{1+ax+bx^2}, \\ \dfrac{dy}{dt} = \dfrac{c\beta xy}{1+ax+bx^2} - dy, \end{cases} \quad x \neq A, \tag{4.1}$$

$$\begin{cases} x^+ = (1-l_1)x, \\ y^+ = (1-l_2)y + \tau, \end{cases} \quad x = A, \tag{4.2}$$

where $0 < l_1, l_2 < 1$. Here, l_1 is the reduction proportion of the prey population, l_2 is the loss proportion of the predator population during intervention, $\tau > 0$ is the supplemental number of predators, and $A > 0$ is the critical prey density triggering the impulse. Let $y^+ = \sigma(y)$, where $\sigma(y) = (1-l_2)y + \tau$. Systems (4.1) and (4.2) are defined in the nonnegative quadrant R_+^2.

4.1. Impulsive set and phase set

In the single-root stable case, $x_1 < K \le x_2$, and hence only $x = x_1$ lies in the feasible region $x < K$. Therefore, the isoclines are $x = x_1$ and $y = \varphi(x) = \frac{-\beta + \sqrt{\beta^2 + 4\beta kr\left(1+ax+bx^2\right)\left(1-\frac{x}{K}\right)}}{2\beta k}$. The positive equilibrium

$E_1^* = \left(x_1, y_1^*\right)$ is their intersection, where $y_1^* = \varphi(x_1)$. Let L_1 denote the line $x = x_1$, and let L_2 denote the curve $y = \frac{-\beta + \sqrt{\beta^2 + 4\beta k r\left(1+ax+bx^2\right)\left(1-\frac{x}{K}\right)}}{2\beta k}$.

The impulsive set and phase set are defined as $M = \left\{(x, y) \in R_+^2 \mid x = A,\ y \geq 0\right\}$ and $N = \left\{(x, y) \in R_+^2 \mid x = (1 - l_1) A,\ y \geq 0\right\}$, respectively.

4.2. Existence of periodic solutions

4.2.1. Stability of the semi-trivial periodic solution

We consider the case in which the predator population is identically zero and no predators are released, i.e., $y(t) \equiv 0$ and $\tau = 0$. Then system (4.1) reduces to

$$\begin{cases} \dfrac{dx}{dt} = \dfrac{rx}{1 + k \cdot 0}\left(1 - \dfrac{x}{K}\right) - \dfrac{\beta x \cdot 0}{1 + ax + bx^2} = rx\left(1 - \dfrac{x}{K}\right), \\ \dfrac{dy}{dt} = \dfrac{c\beta x \cdot 0}{1 + ax + bx^2} - d \cdot 0 = 0, \end{cases} \quad x \neq A.$$

The impulsive condition (4.2) becomes

$$\begin{cases} x^+ = (1 - l_1)x, \\ y^+ = 0, \end{cases} \quad x = A.$$

Since $y(t) \equiv 0$, this solution is called a semi-trivial periodic solution, denoted by $(x(t), 0)$, where $x(t)$ satisfies the above piecewise differential equation together with the impulsive condition.

Let T be the time interval between two consecutive impulses. At the impulse times $t = nT$ ($n = 0, 1, 2, \ldots$), we have $x(nT) = A$. After the impulse, the prey density becomes

$$x\left(nT^+\right) = (1 - l_1) A \triangleq x_0.$$

On the interval $[nT, (n + 1)T]$, the system is governed by the logistic equation with the initial value $x\left(nT^+\right) = x_0$. Its solution is

$$x(t) = \frac{K}{1 + \left(\frac{K}{x_0} - 1\right) e^{-r(t-nT)}}, \quad t \in [nT, (n + 1)T). \tag{4.3}$$

After time T, the prey density reaches A again. Substituting $x\left((n + 1)T\right) = A$ into (4.3) gives

$$A = \frac{K}{1 + \left(\frac{K}{x_0} - 1\right) e^{-rT}}.$$

Thus, the impulsive period is

$$T = \frac{1}{r} \ln\left[\frac{A(K - x_0)}{x_0(K - A)}\right].$$

Substituting $x_0 = (1 - l_1) A$ into the above expression, we obtain

$$T = \frac{1}{r} \ln\left[\frac{K - (1 - l_1)A}{(1 - l_1)(K - A)}\right]. \tag{4.4}$$

For biological feasibility, we require $A < K$. Therefore, when $\tau = 0$, systems (4.1) and (4.2) admit a semi-trivial periodic solution

$$\begin{cases} x_T(t) = \dfrac{K}{1 + \left(\dfrac{K}{(1-l_1)A} - 1\right) e^{-r(t-(n-1)T)}}, \quad t \in [(n-1)T, nT], \\ y_T(t) = 0. \end{cases} \tag{4.5}$$

Here, $n = 1, 2, \ldots$, and T is given by (4.4).

Theorem 4.2.1. Suppose that systems (4.1) and (4.2) satisfy $\tau = 0$ and $A < K$. Then the semi-trivial periodic solution $(x_T(t), 0)$ is locally asymptotically stable if and only if $l_2 > l_2^*$, where

$$l_2^* = 1 - \left[\frac{A\,(K - (1-l_1)A)}{(1-l_1)A(K-A)}\right]^{\frac{d}{r}} \exp\left(-\frac{c\beta}{r} \int_{(1-l_1)A}^{A} \frac{dx}{(1 + ax + bx^2)\left(1 - \frac{x}{K}\right)}\right). \tag{4.6}$$

If $l_2 < l_2^*$, then the periodic solution is unstable.

Proof. Let

$$P(x, y) = \frac{dx}{dt},\ Q(x, y) = \frac{dy}{dt},$$

and write the impulsive mapping as

$$x^+ = x + \alpha(x, y),\ y^+ = y + \beta(x, y),$$

where $\alpha(x, y) = -l_1 x$ and $\beta(x, y) = -l_2 y$ because $\tau = 0$. The impulsive surface is $\phi(x, y) = x - A = 0$. The semi-trivial periodic solution $(x_T(t), 0)$ satisfies $x_T\,(0^+) = (1 - l_1)\,A$, $x_T(T) = A$, and $y_T(t) \equiv 0$. The Floquet multiplier μ is

$$\mu = \Delta_1 \exp\left(\int_0^T \left(\frac{\partial P}{\partial x}(x_T(t), 0) + \frac{\partial Q}{\partial y}(x_T(t), 0)\right) dt\right), \tag{4.7}$$

where

$$\Delta_1 = \left.\frac{P\left(\frac{\partial\beta}{\partial y}\frac{\partial\phi}{\partial x} - \frac{\partial\beta}{\partial x}\frac{\partial\phi}{\partial y} + \frac{\partial\phi}{\partial x}\right) + Q\left(\frac{\partial\alpha}{\partial y}\frac{\partial\phi}{\partial x} - \frac{\partial\alpha}{\partial x}\frac{\partial\phi}{\partial y} + \frac{\partial\phi}{\partial y}\right)}{P\frac{\partial\phi}{\partial x} + Q\frac{\partial\phi}{\partial y}}\right|_{(A,0)} \cdot \frac{P((1-l_1)A, 0)}{P(A, 0)}. \tag{4.8}$$

At $(A, 0)$,

$$P(A, 0) = rA\left(1 - \frac{A}{K}\right),\ Q(A, 0) = 0.$$

Moreover,

$$\frac{\partial\alpha}{\partial x} = -l_1,\ \frac{\partial\alpha}{\partial y} = 0,\ \frac{\partial\beta}{\partial x} = 0,\ \frac{\partial\beta}{\partial y} = -l_2,\ \frac{\partial\phi}{\partial x} = 1,\ \frac{\partial\phi}{\partial y} = 0.$$

At $((1 - l_1)\,A, 0)$,

$$P\,((1 - l_1)\,A, 0) = r\,(1 - l_1)\,A\left(1 - \frac{(1 - l_1)\,A}{K}\right).$$

Substituting these expressions into (4.8) yields

$$\Delta_1 = (1 - l_2)\frac{(1 - l_1)(K - (1 - l_1)A)}{K - A}. \tag{4.9}$$

Along $(x_T(t), 0)$,

$$\frac{\partial P}{\partial x}(x, 0) = r\left(1 - \frac{2x}{K}\right), \ \frac{\partial Q}{\partial y}(x, 0) = \frac{c\beta x}{1 + ax + bx^2} - d.$$

Hence,

$$\int_0^T \left(\frac{\partial P}{\partial x} + \frac{\partial Q}{\partial y}\right)dt = \int_0^T r\left(1 - \frac{2x_T}{K}\right)dt + \int_0^T \frac{c\beta x_T}{1 + ax_T + bx_T^2}dt - dT. \tag{4.10}$$

Since $\frac{dx}{dt} = rx_T\left(1 - \frac{x_T}{K}\right)$, the first integral becomes

$$\int_0^T r\left(1 - \frac{2x_T}{K}\right)dt = \int_{(1-l_1)A}^{A}\left(\frac{1}{x} - \frac{1}{K - x}\right)dx = \ln\frac{A(K - A)}{(1 - l_1)A\left[K - (1 - l_1)A\right]}. \tag{4.11}$$

Similarly,

$$\int_0^T \frac{c\beta x_T}{1 + ax_T + bx_T^2}dt = \frac{c\beta}{r}\int_{(1-l_1)A}^{A}\frac{dx}{(1 + ax + bx^2)\left(1 - \frac{x}{K}\right)}. \tag{4.12}$$

From (4.4),

$$e^{-dT} = \left[\frac{(1 - l_1)A(K - A)}{A\left(K - (1 - l_1)A\right)}\right]^{\frac{d}{r}}. \tag{4.13}$$

Substituting (4.9), (4.11), (4.12), and (4.13) into (4.7) gives

$$\mu = (1 - l_2)\left[\frac{(1 - l_1)A(K - A)}{A\left(K - (1 - l_1)A\right)}\right]^{\frac{d}{r}}\exp\left(\frac{c\beta}{r}\int_{(1-l_1)A}^{A}\frac{dx}{(1 + ax + bx^2)\left(1 - \frac{x}{K}\right)}\right). \tag{4.14}$$

Since $\mu > 0$, Lemma 2.1 implies that the semi-trivial periodic solution is locally asymptotically stable if and only if $\mu < 1$ and is unstable if $\mu > 1$. Setting $\mu = 1$ gives the critical value l_2^* in (4.6). From (4.14), μ decreases monotonically with respect to l_2. Therefore, $\mu < 1$ for $l_2 > l_2^*$, and $\mu > 1$ for $l_2 < l_2^*$. □

4.2.2. Existence of order-one periodic solutions

The relative positions of the impulsive set and the phase set lead to the following cases.
When $A > x_1$, let R be the intersection point between the impulsive set M and the curve L_2. The trajectory through R, denoted by τ_1, intersects L_2 at two points, R and Q.
Case 1. If $(1 - l_1)A \geq x_Q$, let G_2 and G_1 be the two intersection points between τ_1 and the phase set N.

(a) If $\sigma(y_R) = y_{G_2}$, then G_2 is a fixed point, and an order-one periodic solution exists. If $\sigma(y_R) = y_{G_1}$, then an order-one periodic solution also exists, as illustrated in Figure 3(a).

(b) If $\sigma(y_R) > y_{G_2}$, let G_3 denote the post-impulse point of R, with $y_{G_3} = \sigma(y_R)$. Then G_3 is the successor of G_2, and $F(G_2) = y_{G_3} - y_{G_2} = \sigma(y_R) - y_{G_2} > 0$. The trajectory starting from G_3 reaches

the impulsive set at R_1, where $y_R > y_{R_1}$. Since $\sigma(y)$ is increasing, $\sigma(y_{R_1}) < \sigma(y_R)$. Let G_4 be the post-impulse point of R_1. Then G_4 is the successor of G_3, and $F(G_3) = y_{G_4} - y_{G_3} = \sigma(y_{R_1}) - \sigma(y_R) < 0$. By the continuity of the successor function, there exists a point G_k such that $F(G_k) = 0$. Hence, an order-one periodic solution exists, as illustrated in Figure 3(b).

(c) If $y_{G_1} < \sigma(y_R) < y_{G_2}$, then the post-impulse point of R cannot reach the impulsive set again and approaches the equilibrium, as illustrated in Figure 3(c).

(d) If $\sigma(y_R) < y_{G_1}$, let G_5 be the post-impulse point of R, with $y_{G_5} = \sigma(y_R)$. Then G_5 is the successor of G_1, and $F(G_1) = y_{G_5} - y_{G_1} < 0$. Choose a point G_6 on N whose ordinate is smaller than τ. Let the trajectory through G_6 reach the impulsive M at R_2. Since $y_{R_2} \geq 0$, the post-impulse point G_7 satisfies $y_{G_7} > \tau > y_{G_6}$, and hence $F(G_6) > 0$. By continuity, there exists G_k such that $F(G_k) = 0$. Thus, an order-one periodic solution exists, as shown in Figure 3(d).

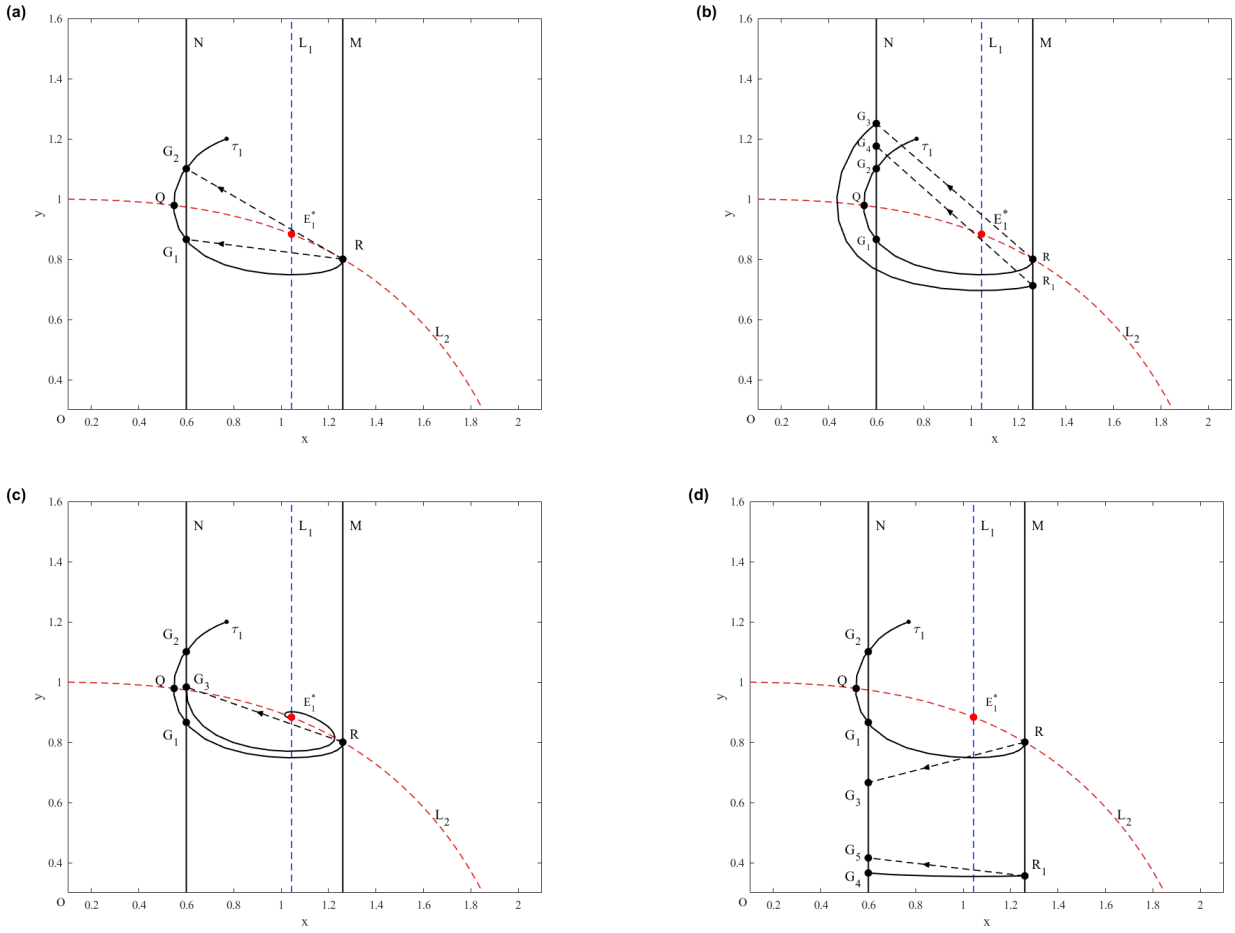

Figure 3. Existence of order-one periodic solutions under unilateral impulsive control when the threshold exceeds the equilibrium prey density. Four subcases illustrate the successor function method. Parameter values: $r = 2$, $K = 2$, $k = 1$, $\beta = 1$, $a = 0.5$, $b = 0.2$, $c = 0.5$, $d = 0.3$, $A = 1.118$, $l_1 = 0.25$, $l_2 = 0.2$, $\tau = 0.9$.

Case 2. If $(1 - l_1)A < x_Q$, the phase set N does not intersect the trajectory τ_1. Let E be the intersection point between N and L_2. The trajectory through E, denoted by τ_2, intersects M at F, as illustrated in

Figure 4.
(a) If $\sigma(y_F) = y_E$, then E is a fixed point, and an order-one periodic solution exists.
(b) If $\sigma(y_F) > y_E$, the proof is analogous to that of Case 1(b).
(c) If $\sigma(y_F) < y_E$, the proof is analogous to that of Case 1(d).

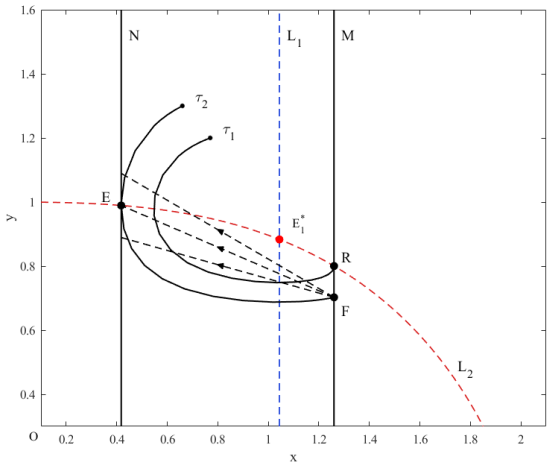

Figure 4. Existence of order-one periodic solutions under unilateral impulsive control when the phase set does not intersect the trajectory in Case 2. Parameter values are the same as in Figure 3.

Case 3. If $A < x_1$, let E be the intersection point between N and L_2. The trajectory through E intersects the impulsive set at F. As in Case 2, there always exists an order-one periodic solution.

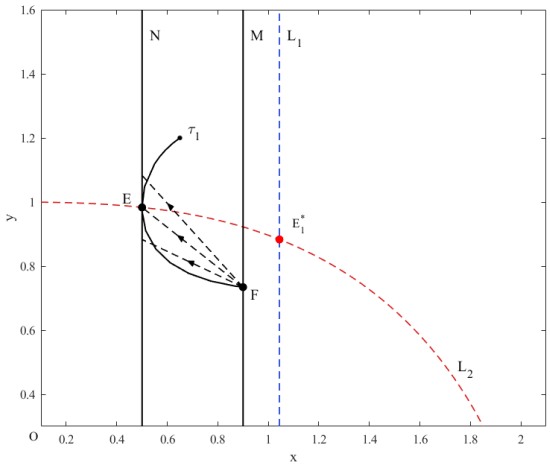

Figure 5. Existence of order-one periodic solutions under unilateral impulsive control when the threshold is below the equilibrium prey density. Parameter values are the same as in Figure 3, with $A = 0.8$.

4.2.3. Stability of order-one periodic solutions

Theorem 4.2.2. Suppose that systems (4.1) and (4.2) admit an order-one periodic solution $\Gamma(t) = \left(x_p(t), y_p(t)\right)$ with period $T > 0$, which intersects the impulsive set M exactly once during one period at $I = \left(A, y_p\right)$. The impulsive mapping sends I to the post-impulse point $J = \left((1 - l_1)A,\ (1 - l_2)y_p + \tau\right)$ in the phase set N. Then $\Gamma(t)$ is locally orbitally asymptotically stable if and only if

$$l_1 > l_1^* \triangleq 1 - \frac{f(I)}{f(J)} \cdot \exp\left(-\int_0^T \left(\frac{\partial f}{\partial x}(\Gamma(t)) + \frac{\partial g}{\partial y}(\Gamma(t))\right)dt\right). \tag{4.15}$$

If $l_1 < l_1^*$, then the periodic solution is unstable.

Proof. Let

$$f(x, y) = \frac{rx}{1 + ky}\left(1 - \frac{x}{K}\right) - \frac{\beta xy}{1 + ax + bx^2},\ g(x, y) = \frac{c\beta xy}{1 + ax + bx^2} - dy.$$

The orbital stability of $\Gamma(t)$ is determined by the Floquet multiplier

$$\mu = \Delta_1 \cdot \exp\left(\int_0^T \left(\frac{\partial f}{\partial x}(\Gamma(t)) + \frac{\partial g}{\partial y}(\Gamma(t))\right)dt\right), \tag{4.16}$$

where

$$\Delta_1 = \left.\frac{\left(\frac{\partial \phi}{\partial x}\frac{\partial \Phi_1}{\partial x} + \frac{\partial \phi}{\partial y}\frac{\partial \Phi_1}{\partial y}\right)f + \left(\frac{\partial \phi}{\partial x}\frac{\partial \Phi_2}{\partial x} + \frac{\partial \phi}{\partial y}\frac{\partial \Phi_2}{\partial y}\right)g}{f\frac{\partial \phi}{\partial x} + g\frac{\partial \phi}{\partial y}}\right|_I \cdot \frac{f(\Phi(I))}{f(I)}. \tag{4.17}$$

Here, $\phi(x, y) = x - A = 0$, $\Phi_1(x, y) = (1 - l_1)x$, and $\Phi_2(x, y) = (1 - l_2)y + \tau$. At $I = \left(A, y_p\right)$,

$$\frac{\partial \phi}{\partial x} = 1,\ \frac{\partial \phi}{\partial y} = 0,\ \frac{\partial \Phi_1}{\partial x} = 1 - l_1,\ \frac{\partial \Phi_1}{\partial y} = 0,\ \frac{\partial \Phi_2}{\partial x} = 0,\ \frac{\partial \Phi_2}{\partial y} = 1 - l_2.$$

Substituting these derivatives into (4.17) gives

$$\Delta_1 = (1 - l_1)\frac{f(\Phi(I))}{f(I)} = (1 - l_1)\frac{f(J)}{f(I)}. \tag{4.18}$$

Thus,

$$\mu = (1 - l_1)\frac{f(J)}{f(I)} \exp\left(\int_0^T \left(\frac{\partial f}{\partial x}(\Gamma(t)) + \frac{\partial g}{\partial y}(\Gamma(t))\right)dt\right). \tag{4.19}$$

Setting $\mu = 1$ gives

$$l_1^* = 1 - \frac{f(I)}{f(J)} \cdot \exp\left(-\int_0^T \left(\frac{\partial f}{\partial x}(\Gamma(t)) + \frac{\partial g}{\partial y}(\Gamma(t))\right)dt\right).$$

According to Lemma 2.1, $\Gamma(t)$ is locally orbitally asymptotically stable if and only if $\mu < 1$, which is equivalent to $l_1 > l_1^*$. The periodic solution is unstable when $l_1 < l_1^*$. □

5. Complex dynamics analysis under bilateral impulsive control

For system (2.1), we again consider the single-root stable case in which $\beta > \beta_2,\ x_1 < K \le x_2$, and $K < \frac{1+2ax_1+3bx_1^2}{a+2bx_1}$ and assume that the positive equilibrium is a stable focus. To prevent both pest outbreaks and non-target ecological risks caused by excessive natural enemies, we introduce a low threshold L and a high threshold H. When the aphid density decreases to the low threshold L, it is already below the economically harmful range. Continuing to maintain a high density of harlequin ladybirds under prey scarcity may increase competition, dispersal, and potential non-target effects. Therefore, the low-threshold action reduces the active natural-enemy population according to $y^+ = (1-\mu)y$. The relation $x^+ = x + \delta$ does not represent the deliberate release of aphids; rather, δ describes a small effective recovery of the surviving aphid population after intensive control is relaxed, including rapid reproduction and redistribution from untreated plant parts [27–29]. The parameter δ is restricted so that $L + \delta$ remains within the safe management interval. At the high threshold $x = H$, the opposite action $x^+ = x - \eta$ and $y^+ = (1+\nu)y$ represents direct aphid reduction together with supplementation of harlequin ladybirds [19, 20, 22]. The two threshold actions therefore form a biologically interpretable buffer that avoids both aphid outbreaks and excessive natural-enemy pressure. This leads to the following bilateral state-feedback impulsive model:

$$\begin{cases} \dfrac{dx}{dt} = \dfrac{rx}{1+ky}\left(1-\dfrac{x}{K}\right) - \dfrac{\beta xy}{1+ax+bx^2}, \\ \dfrac{dy}{dt} = \dfrac{c\beta xy}{1+ax+bx^2} - dy, \end{cases} \qquad L < x < H. \tag{5.1}$$

Low-threshold impulse:

$$\begin{cases} x^+ = x + \delta, \\ y^+ = (1-\mu)y, \end{cases} \qquad x = L. \tag{5.2}$$

High-threshold impulse:

$$\begin{cases} x^+ = x - \eta, \\ y^+ = (1+\nu)y, \end{cases} \qquad x = H. \tag{5.3}$$

Here, $0 < L < x_1 < H < K$, $\delta > 0$ with $L + \delta < H$, and $\eta > 0$ with $H - \eta > L$. The parameter $\mu > 0$ represents the proportional reduction in the predator population at the low threshold, and $\nu > 0$ represents the proportional increase in the predator population at the high threshold. The quantity δ represents the short-term compensatory recovery of pests within the safe range after intensive control is relaxed [27–29], whereas η denotes the amount of pest removal. For the numerical case considered below, $x_1 \approx 1.044$, $L = 0.72$, $\delta = 0.04$, and $H = 1.10$; hence, $L + \delta = 0.76 < x_1 < H$, so the modeled recovery remains well below the upper intervention threshold. The purpose of this bilateral strategy is to keep the pest–natural enemy system within a reasonable management range.

5.1. Definitions of impulsive sets and phase sets

Because both low-threshold and high-threshold impulses are involved, two impulsive sets and their corresponding phase sets are defined separately. The low-threshold impulsive set is

$$M_L = \left\{(x,y) \in R_+^2 : x = L,\ y \ge 0\right\}.$$

After an impulse occurs on M_L, the state jumps to the low-threshold phase set

$$N_L = \left\{(x, y) \in R_+^2 : x = L + \delta,\ y \geq 0\right\}.$$

Similarly, the high-threshold impulsive set is

$$M_H = \left\{(x, y) \in R_+^2 : x = H,\ y \geq 0\right\},$$

and the corresponding phase set is

$$N_H = \left\{(x, y) \in R_+^2 : x = H - \eta,\ y \geq 0\right\}.$$

The low-threshold impulsive mapping $\phi_L : M_L \to N_L$ is defined by $\phi_L(L, y) = (L + \delta,\ (1 - \mu)y)$. The high-threshold impulsive mapping $\phi_H : M_H \to N_H$ is defined by $\phi_H(H, y) = (H - \eta,\ (1 + \nu)y)$.

In this section, we focus on the configuration

$$L + \delta < x_1 < H - \eta.$$

In this configuration, the post-impulse state generated at the low threshold lies to the left of the stable equilibrium, whereas the post-impulse state generated at the high threshold lies to its right. This straddling arrangement allows the trajectory to alternate between the two threshold surfaces and is the configuration considered in the following existence and stability analysis.

5.2. Existence of periodic solutions

Let F_1 and F_2 denote the intersections of the isocline $\varphi(x_1)$ with M_L and M_H, respectively. The trajectory through F_1 intersects N_H at $F_1^{'}$, and the trajectory through F_2 intersects N_L at $F_2^{'}$. The post-impulse point of F_1 after the low-threshold impulse is denoted by F_1^+, and the post-impulse point of F_2 after the high-threshold impulse is denoted by F_2^+. Since $F_1^{'}$ lies on N_H and $F_2^{'}$ lies on N_L, the corresponding pre-impulse points on M_H and M_L can be identified and denoted by F_4 and F_3, respectively.

Theorem 5.1. Assume that $L+\delta < x_1 < H-\eta$. If $\nu \gg \frac{y_{F_1'}}{y_{F_2}} - 1$ and $\frac{y_{F_2'}}{y_{F_1}} \ll \mu < 1$, then systems (5.1)–(5.3) admit a bilateral order-one periodic solution. Here, $y_{F_2} = \varphi(H)$ and $y_{F_1} = \varphi(L)$.

Proof. Suppose that $\nu \gg \frac{y_{F_1'}}{y_{F_2}} - 1$, namely $y_{F_2^+} \gg y_{F_1'}$. We choose a point B_1 such that $0 < y_{F_2'} - y_{B_1} < \varepsilon$. The trajectory through B_1 intersects M_H at B_2, which lies below F_2 and is arbitrarily close to it. After the high-threshold impulse, B_2 jumps to $B_3 \in N_H$, with $y_{B_3} \gg y_{F_1'}$. The trajectory through B_3 intersects M_L at B_4, and since $y_{B_4} \gg y_{F_1}$, we have $y_{B_4} > y_{F_3}$. After the low-threshold impulse, B_4 jumps to $B_5 \in N_L$, and $y_{B_5} > y_{F_2'} > y_{B_1}$. Thus, $F(B_1) > 0$, as illustrated in Figure 6(a).

If $\frac{y_{F_2'}}{y_{F_1}} \ll \mu < 1$, namely $y_{F_1^+} \ll y_{F_2'}$, let C_1 be a point on N_L such that the trajectory through C_1 intersects M_H at C_2, where $0 < y_{C_2} - y_{F_4} < \varepsilon$. After the high-threshold impulse, C_2 jumps to $C_3 \in N_H$, which approaches $F_1^{'}$. The trajectory through C_3 intersects M_L at C_4, and after the low-threshold impulse, C_4 jumps to $C_5 \in N_L$. Then C_5 approaches F_1. Since $y_{F_1^+} \ll y_{F_2'}$, we have $y_{C_5} < y_{C_1}$. Thus, $F(C_1) < 0$, as illustrated in Figure 6(b).

By the continuity of the successor function, there exists a point $I_* \in N_L$ such that $F(I_*) = 0$. Hence, systems (5.1)–(5.3) admit a bilateral order-one periodic solution under the condition $L + \delta < x_1 < H - \eta$. □

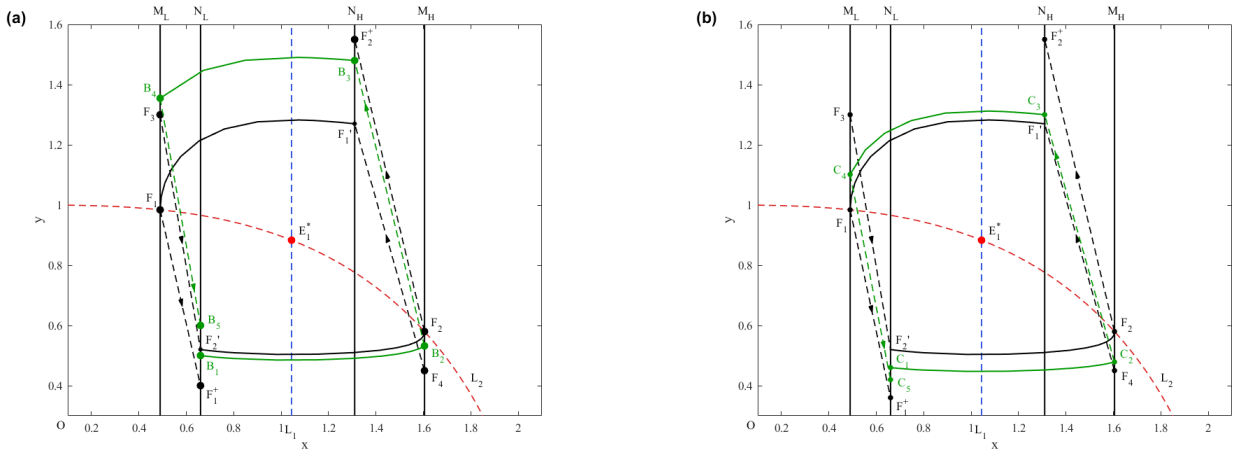

Figure 6. Geometric construction for the existence of a bilateral order-one periodic solution using positive and negative values of the successor function. Parameter values: $r = 2$, $K = 2$, $k = 1$, $\beta = 1$, $a = 0.5$, $b = 0.2$, $c = 0.5$, $d = 0.3$, $L = 0.72$, $H = 1.1$, $\delta = 0.04$, $\eta = 0.03$, $\mu = 0.21$, $\nu = 0.60$.

5.3. Stability of periodic solutions

Theorem 5.2. Suppose that systems (5.1)–(5.3) have a bilateral order-one periodic solution $\Gamma(t) = \left(x_p(t), y_p(t)\right)$ with period $T > 0$. Let its intersections with the low- and high-threshold impulsive sets be $I_L = (L, y_L)$ and $I_H = (H, y_H)$, respectively. The corresponding post-impulse points are

$$J_L = \phi_L(I_L) = (L + \delta,\ (1 - \mu)y_L),\ J_H = \phi_H(I_H) = (H - \eta,\ (1 + \nu)y_H).$$

If

$$\frac{f(J_L)}{f(I_L)} \cdot \frac{f(J_H)}{f(I_H)} \cdot \exp\left(\int_0^T \operatorname{tr} J(\Gamma(t))\, dt\right) < 1,$$

then the periodic solution is locally orbitally asymptotically stable.

Proof. Let

$$f(x, y) = \frac{rx}{1 + ky}\left(1 - \frac{x}{K}\right) - \frac{\beta xy}{1 + ax + bx^2},\ g(x, y) = \frac{c\beta xy}{1 + ax + bx^2} - dy,$$

and let $J(x, y)$ be the corresponding Jacobian matrix, with $\operatorname{tr} J = \frac{\partial f}{\partial x} + \frac{\partial g}{\partial y}$. For a periodic solution with two impulses over one period, the Floquet multiplier can be expressed as the product of the contribution of the continuous flow and the contributions at the impulsive points:

$$\mu = \Delta_L \cdot \Delta_H \cdot \exp\left(\int_0^T \operatorname{tr} J(\Gamma(t))dt\right), \tag{5.4}$$

where Δ_L and Δ_H are the contribution factors at the low and high impulses, respectively. The general formula is

$$\Delta = \left.\frac{\left(\frac{\partial\phi}{\partial x}\frac{\partial\Phi_1}{\partial x} + \frac{\partial\phi}{\partial y}\frac{\partial\Phi_1}{\partial y}\right)f + \left(\frac{\partial\phi}{\partial x}\frac{\partial\Phi_2}{\partial x} + \frac{\partial\phi}{\partial y}\frac{\partial\Phi_2}{\partial y}\right)g}{f\frac{\partial\phi}{\partial x} + g\frac{\partial\phi}{\partial y}}\right|_I \cdot \frac{f(\Phi(I))}{f(I)}. \tag{5.5}$$

For the low impulse, $\phi_L(x, y) = x - L = 0$ and $\Phi_L(x, y) = (x + \delta,\ (1 - \mu)y)$. At $I_L = (L, y_L)$,

$$\frac{\partial \phi_L}{\partial x} = 1,\ \frac{\partial \phi_L}{\partial y} = 0,$$

$$\frac{\partial \Phi_{L1}}{\partial x} = 1,\ \frac{\partial \Phi_{L1}}{\partial y} = 0,\ \frac{\partial \Phi_{L2}}{\partial x} = 0,\ \frac{\partial \Phi_{L2}}{\partial y} = 1 - \mu.$$

Substituting these into (5.5) gives

$$\Delta_L = \frac{f(I_L)}{f(I_L)} \cdot \frac{f(\Phi_L(I_L))}{f(I_L)} = \frac{f(J_L)}{f(I_L)}. \tag{5.6}$$

For the high impulse, $\phi_H(x, y) = x - H = 0$ and $\Phi_H(x, y) = (x - \eta,\ (1 + \nu)y)$. At $I_H = (H, y_H)$,

$$\frac{\partial \phi_H}{\partial x} = 1,\ \frac{\partial \phi_H}{\partial y} = 0,$$

$$\frac{\partial \Phi_{H1}}{\partial x} = 1,\ \frac{\partial \Phi_{H1}}{\partial y} = 0,\ \frac{\partial \Phi_{H2}}{\partial x} = 0,\ \frac{\partial \Phi_{H2}}{\partial y} = 1 + \nu.$$

Substitution into (5.5) yields

$$\Delta_H = \frac{f(I_H)}{f(I_H)} \cdot \frac{f(\Phi_H(I_H))}{f(I_H)} = \frac{f(J_H)}{f(I_H)}. \tag{5.7}$$

Combining (5.6) and (5.7), we obtain

$$\mu = \frac{f(J_L)}{f(I_L)} \cdot \frac{f(J_H)}{f(I_H)} \cdot \exp\left(\int_0^T \operatorname{tr} J(\Gamma(t))dt\right). \tag{5.8}$$

Since the multiplier is positive in this setting, Lemma 2.1 implies that the periodic solution is locally orbitally asymptotically stable if $\mu < 1$. The theorem follows. □

6. Numerical simulations

This section presents numerical simulations to verify the theoretical results and illustrate the effects of fear intensity, group-defense parameters, and state-feedback impulsive control on the system dynamics. First, we consider the non-impulsive system (2.1). With the same parameters as those in Figure 1, the system exhibits a unique stable focus, as illustrated in Figure 7.

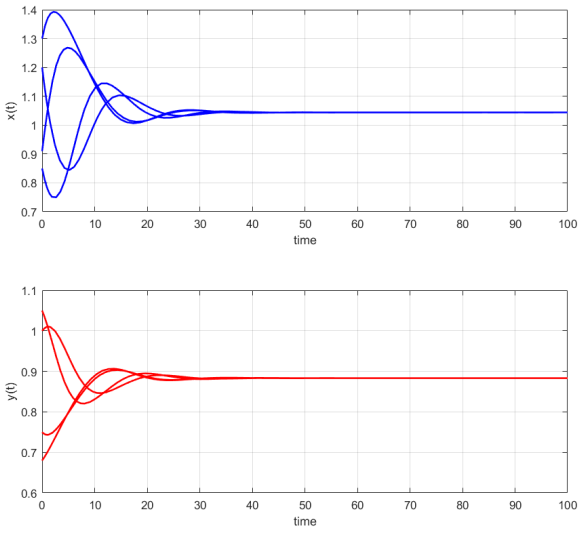

Figure 7. Numerical simulation of the deterministic system showing convergence to the stable-focus equilibrium. Parameter values: $r = 2$, $K = 2$, $k = 1$, $\beta = 1$, $a = 0.5$, $b = 0.2$, $c = 0.5$, $d = 0.3$.

With the same parameters as those in Figure 2, the system has two positive equilibria, namely one stable equilibrium and one saddle point, as illustrated in Figure 8. These results are consistent with the theoretical analysis in Section 3.

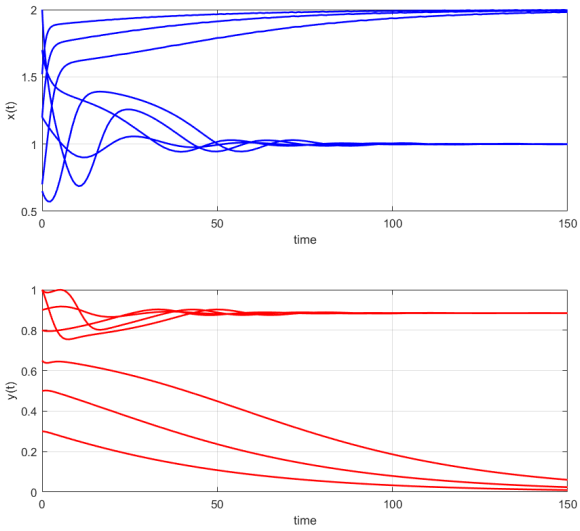

Figure 8. Numerical simulation of the deterministic system confirming one stable equilibrium and one saddle point. Parameter values: $r = 2$, $K = 2$, $k = 1$, $\beta = 1.12$, $a = 0.2$, $b = 2/3$, $c = 0.5$, $d = 0.3$.

Starting from the baseline parameter set given in Figure 1, the fear effect coefficient k, the low-

density defense parameter a, and the high-density defense parameter b were varied to obtain Figures 9–11, respectively. Figure 9 shows that increasing the fear coefficient k suppresses prey reproduction and lowers the predator equilibrium density, while the prey equilibrium determined by the predator nullcline changes only slightly. Figure 10 shows that increasing the low-density group-defense parameter a weakens predation efficiency, shifts the prey equilibrium to a higher level, and reduces the predator level for the parameter range displayed. Figure 11 shows a similar but stronger high-density defense effect when b increases: Prey density rises, predator density declines, and the phase trajectory converges to the corresponding shifted equilibrium. The time-series and phase-plane panels also show that the transient oscillations decay and the trajectories converge to the corresponding equilibria.

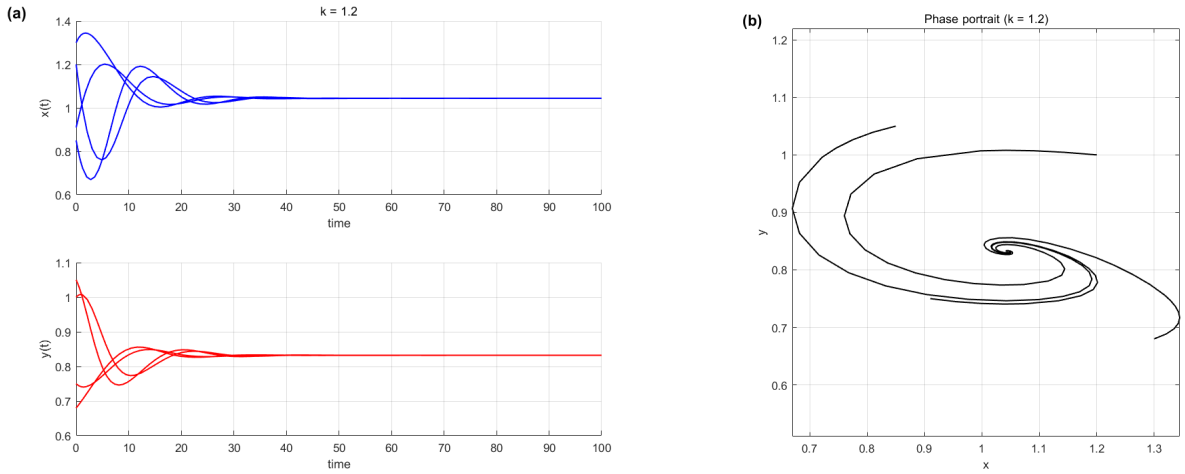

Figure 9. Numerical simulation illustrating the effect of increasing fear intensity on predator density. Parameter values: $r = 2$, $K = 2$, $\beta = 1$, $a = 0.5$, $b = 0.2$, $c = 0.5$, $d = 0.3$; k varies as shown.

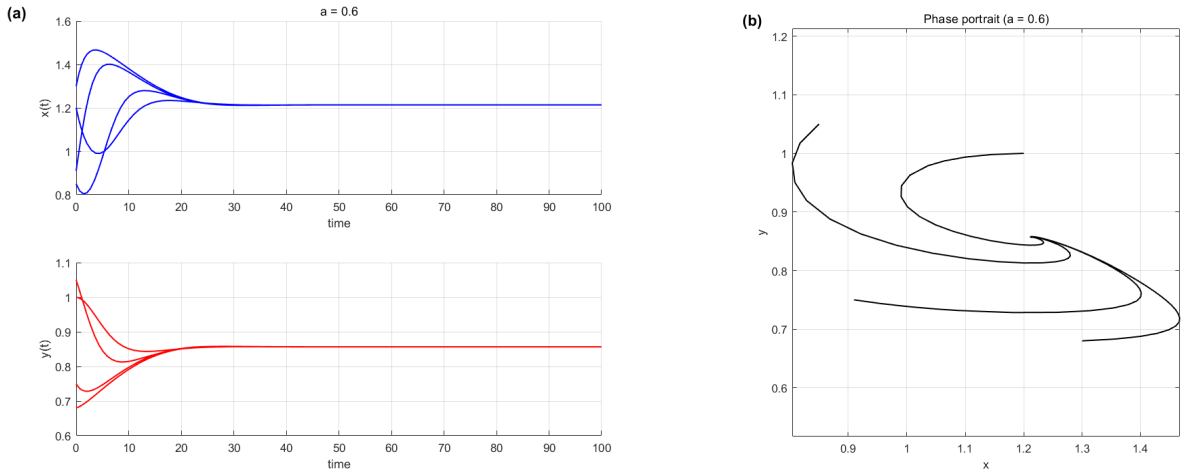

Figure 10. Numerical simulation showing the influence of the low-density defense parameter on population dynamics. Parameter values: $r = 2$, $K = 2$, $k = 1$, $\beta = 1$, $b = 0.2$, $c = 0.5$, $d = 0.3$; a varies as shown.

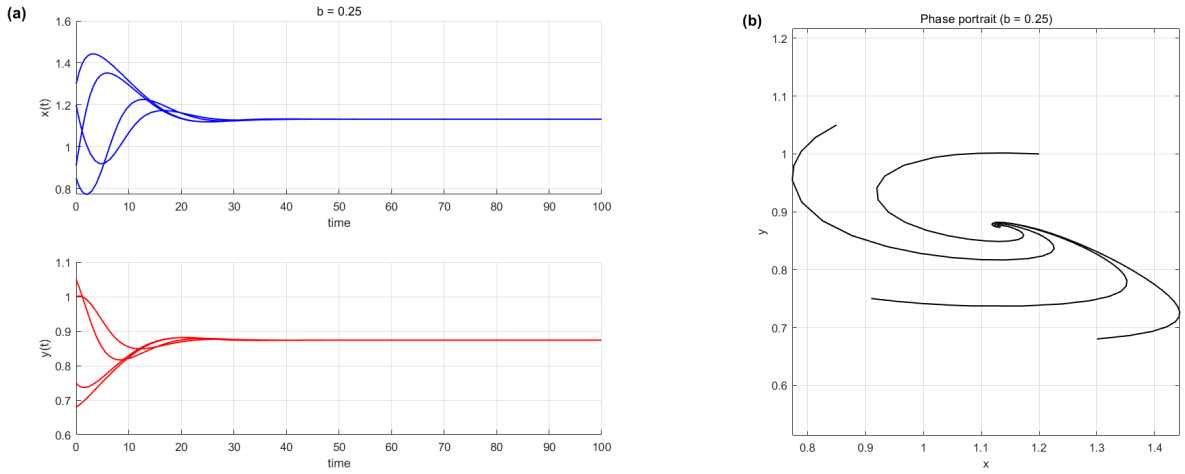

Figure 11. Numerical simulation demonstrating the impact of the high-density defense parameter on prey and predator densities. Parameter values: $r = 2$, $K = 2$, $k = 1$, $\beta = 1$, $a = 0.5$, $c = 0.5$, $d = 0.3$; b varies as shown.

Next, we consider the unilateral state-feedback impulsive control strategy. The continuous parameters are the same as those in Figure 1, and the impulsive parameters are given in the caption of Figure 12. As shown in Figure 12, after a short transient phase, the system exhibits stable periodic oscillations, and the phase trajectory forms a closed structure between the impulsive set and the phase set. This supports the existence and stability of the unilateral order-one periodic solution. Biologically, this result suggests that reducing pests and supplementing natural enemies when aphids reach the economic threshold can effectively regulate the system [19, 22].

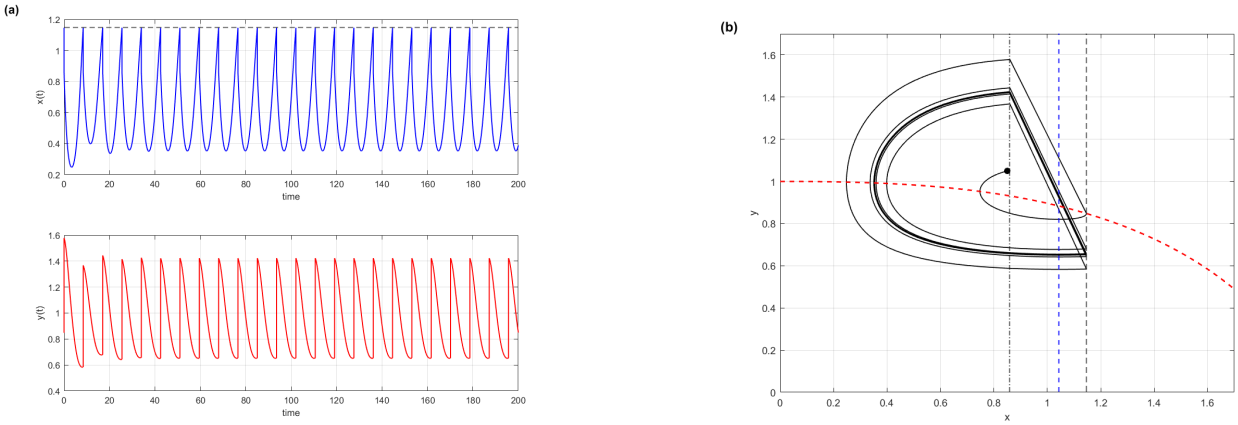

Figure 12. Numerical simulation of the unilateral impulsive system showing a stable order-one periodic orbit after a transient phase. Parameter values: $r = 2$, $K = 2$, $k = 1$, $\beta = 1$, $a = 0.5$, $b = 0.2$, $c = 0.5$, $d = 0.3$, $A = 1.118$, $l_1 = 0.25$, $l_2 = 0.2$, $\tau = 0.9$.

Finally, we consider the bilateral state-feedback impulsive control strategy. The continuous parameters are the same as those in Figure 1, and the thresholds and impulsive parameters are given in the caption of Figure 13. This parameter set satisfies the geometric conditions for the existence

of a bilateral order-one periodic solution. Figure 13 shows that the prey and predator populations eventually settle into stable periodic oscillations. The trajectory moves repeatedly between the low- and high-threshold impulsive sets and their corresponding phase sets, forming a stable bilateral order-one periodic solution.

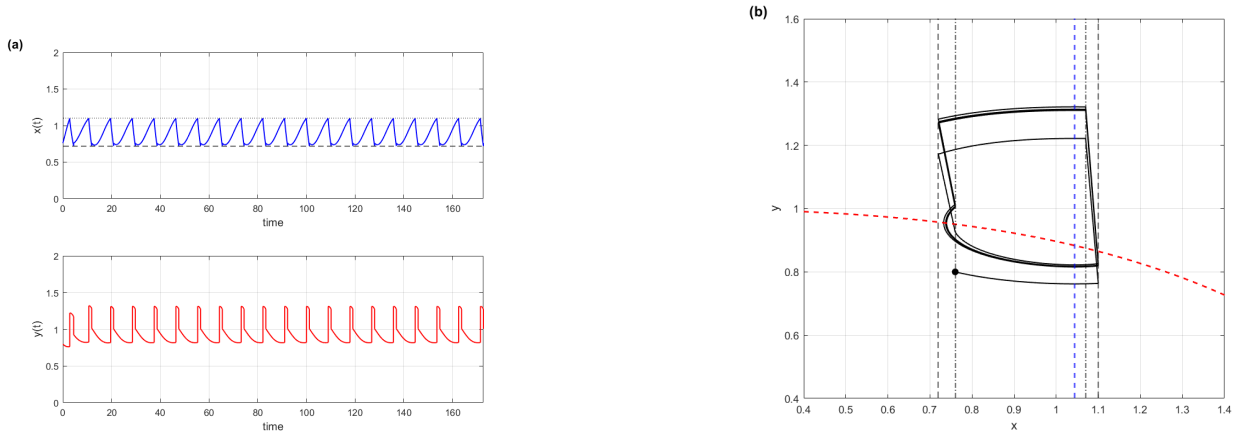

Figure 13. Numerical simulation of the bilateral impulsive system exhibiting a stable bilateral order-one periodic solution. Parameter values: $r = 2$, $K = 2$, $k = 1$, $\beta = 1$, $a = 0.5$, $b = 0.2$, $c = 0.5$, $d = 0.3$, $L = 0.72$, $H = 1.1$, $\delta = 0.04$, $\eta = 0.03$, $\mu = 0.21$, $\nu = 0.60$.

To examine the attractivity of this periodic orbit, three representative initial points are selected: $P_1 = (1.06, 0.72)$, $P_2 = (0.66, 0.95)$, and $P_3 = (1.18, 0.75)$. These points are not located on the impulsive sets $x = L$ and $x = H$ or on the phase sets $x = L + \delta$ and $x = H - \eta$. In the simulations, the trajectories first evolve according to the continuous dynamics and then undergo impulses after reaching the corresponding thresholds. Figure 14 shows that, although different initial points produce different transient behaviors, the corresponding trajectories eventually converge to the same stable bilateral periodic orbit. This indicates that the periodic solution has strong attractivity and a certain degree of robustness.

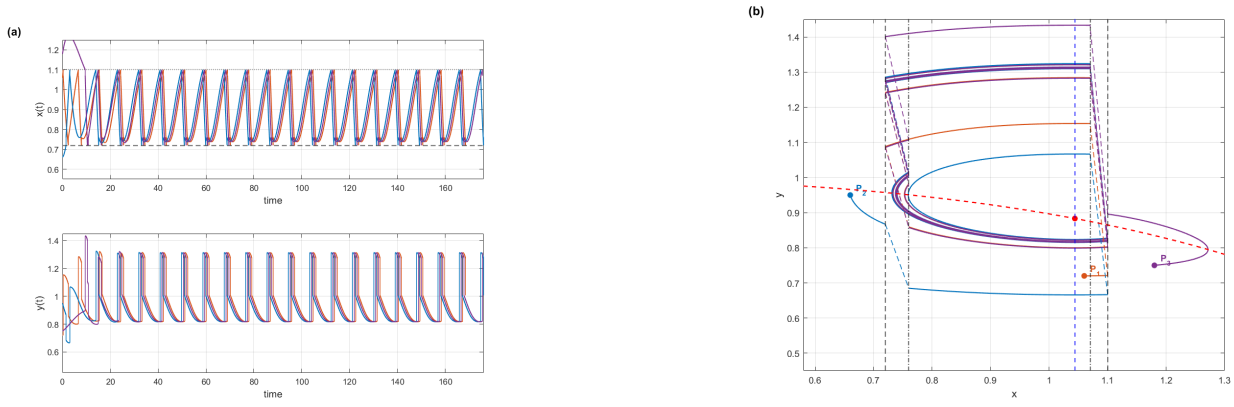

Figure 14. Dynamic behavior of the bilateral impulsive control strategy, which maintains prey and predator populations within an ecologically safe range. Parameter values are the same as in Figure 13.

From a biological perspective, bilateral impulsive control does not aim to eliminate aphids but rather aims to maintain them near the safe range determined by L and H [22]. When aphids reach the high threshold, the system suppresses outbreaks by reducing pests and enhancing the effect of predators. When aphid density decreases to the low threshold, the system reduces predator pressure and allows short-term pest recovery [27–29], thereby avoiding non-target ecological risks caused by excessive natural enemies. Thus, the strategy reflects a balance between pest control and ecological stability.

7. Results

For the non-impulsive system, the positivity and boundedness of solutions, as well as the existence of equilibria, were rigorously established. The system always possesses two boundary equilibria: E_0, which is a saddle point, and E_K, which is locally asymptotically stable under the corresponding stability condition and is a saddle point otherwise. Positive interior equilibria exist only when the predation rate exceeds a critical threshold. Depending on parameter values, the system may exhibit either a unique positive equilibrium or two distinct positive equilibria. In the latter case, the larger equilibrium is always a saddle point, whereas the smaller equilibrium may be stable or unstable, with a Hopf bifurcation occurring at a critical carrying capacity. Numerical simulations confirm these theoretical findings and further reveal that increasing fear intensity reduces predator density, whereas strengthening group defense leads to higher prey density and lower predator density, indicating that collective defense weakens top-down control. When the natural stable equilibrium fails to meet management goals, a unilateral state-feedback impulsive control strategy is designed. The existence of unilateral order-one periodic solutions is established by the successor function method, while the bilateral existence result is established under the straddling configuration $L + \delta < x_1 < H - \eta$. A criterion for orbital asymptotic stability is derived using the Floquet multiplier. Numerical simulations demonstrate that the system converges to a stable order-one periodic orbit after a short transient phase. To address both pest outbreaks and ecological risks from excessive natural enemies, a bilateral impulsive strategy with low and high thresholds is further developed. The existence and stability of bilateral order-one periodic solutions are established. Numerical simulations confirm that the system can be maintained within an ecologically safe range, and trajectories from different initial conditions converge to the same stable periodic orbit.

8. Discussion and conclusions

The findings provide a deeper understanding of how the fear effect and group defense jointly shape predator–prey dynamics and how state-feedback impulsive control can be used for ecological regulation. The observation that stronger group defense increases prey equilibrium density while reducing predator density is consistent with the classical view that collective protection can buffer predation pressure. This implies that natural enemies may be insufficient to control pest outbreaks when prey exhibit strong group defense, thereby necessitating external intervention. The unilateral impulsive strategy provides an effective means to suppress outbreaks. In contrast, the bilateral strategy introduces a low threshold at which predator pressure is reduced when pests become scarce, thereby preventing natural enemies from attacking non-target organisms or becoming invasive. This concern is particularly relevant for biological control agents such as the harlequin ladybird. Compared with traditional

integrated pest management models that often use only a single high threshold, the bilateral approach offers a more balanced solution that simultaneously considers pest suppression and ecological safety. The theoretical tools employed—the successor function method and impulsive Floquet theory—are effective for studying the existence and stability of periodic solutions. The limitations of this study include the assumptions of deterministic dynamics and instantaneous impulse implementation, as well as the simplified representation of the fear effect. Future studies could incorporate stochastic perturbations, time delays, or optimal control strategies. In particular, future work will investigate the Hopf bifurcation associated with the critical carrying capacity identified in the stability analysis, changes in the number and stability of positive equilibria as key parameters vary, and bifurcations of periodic solutions induced by the impulsive thresholds and control parameters. Despite these limitations, the results provide a theoretical basis for designing state-feedback impulsive control in predator–prey systems where the fear effect and group defense play significant roles.

In conclusion, from an applied perspective, the model can be used to interpret the integrated regulation of aphids and harlequin ladybirds in systems where natural enemies may produce secondary ecological risks. The unilateral impulsive strategy is suitable for rapid control after pests reach the economic threshold, whereas the bilateral impulsive strategy further accounts for potential non-target effects caused by excessive natural enemies when pest density is too low. Therefore, an appropriate management objective is not simply to eradicate pests but to balance pest suppression with ecological risks associated with natural enemies and to maintain both populations within an acceptable dynamic range.

Use of AI tools declaration

The authors declare they have not used Artificial Intelligence (AI) tools in the creation of this article.

Acknowledgments

Meng Zhang was supported by NSFC (no. 11701026).

Conflict of interest

The authors declare that there are no conflicts of interest.

References

1. L. Y. Zanette, A. F. White, M. C. Allen, M. Clinchy, Perceived predation risk reduces the number of offspring songbirds produce per year, *Science*, **334** (2011), 1398–1401. https://doi.org/10.1126/science.1210908
2. E. L. Preisser, D. I. Bolnick, M. F. Benard, Scared to death? The effects of intimidation and consumption in predator-prey interactions, *Ecology*, **86** (2005), 501–509. https://doi.org/10.1890/04-0719
3. M. Clinchy, M. J. Sheriff, L. Y. Zanette, Predator-induced stress and the ecology of fear, *Funct. Ecol.*, **27** (2013), 56–65. https://doi.org/10.1111/1365-2435.12007

4. E. H. Nelson, C. E. Matthews, J. A. Rosenheim, Predators reduce prey population growth by inducing changes in prey behavior, *Ecology*, **85** (2004), 1853–1858. https://doi.org/10.1890/03-3109
5. S. K. Sasmal, Population dynamics with multiple Allee effects induced by fear factors: A mathematical study on prey-predator interactions, *Appl. Math. Modell.*, **64** (2018), 1–14. https://doi.org/10.1016/j.apm.2018.07.021
6. X. Wang, L. Zanette, X. Zou, Modelling the fear effect in predator-prey interactions, *J. Math. Biol.*, **73** (2016), 1179–1204. https://doi.org/10.1007/s00285-016-0989-1
7. J. P. Suraci, M. Clinchy, L. M. Dill, D. Roberts, L. Y. Zanette, Fear of large carnivores causes a trophic cascade, *Nat. Commun.*, **7** (2016), 10698. https://doi.org/10.1038/ncomms10698
8. M. Hartbauer, Collective Defense of *Aphis nerii* and *Uroleucon hypochoeridis* (Homoptera, Aphididae) against Natural Enemies, *PLoS One*, **5** (2010), e10417. https://doi.org/10.1371/journal.pone.0010417
9. G. M. Wu, G. Boivin, J. Brodeur, L. A. Giraldeau, Y. Outreman, Altruistic defence behaviours in aphids, *BMC Evol. Biol.*, **10** (2010), 19. https://doi.org/10.1186/1471-2148-10-19
10. C. Holling, The components of predation as revealed by a study of small-mammal predation of the European pine sawfly, *Can. Entomol.*, **91** (1959), 293–320. https://doi.org/10.4039/Ent91293-5
11. M. L. Rosenzweig, R. H. MacArthur, Graphical representation and stability conditions of predator-prey interactions, *Am. Nat.*, **97** (1963), 209–223. https://doi.org/10.1086/282272
12. H. I. Freedman, G. S. K. Wolkowicz, Predator-prey systems with group defence: the paradox of enrichment revisited, *Bull. Math. Biol.*, **48** (1986), 493–508. https://doi.org/10.1007/BF02462320
13. J. B. Collings, The effects of the functional response on the bifurcation behavior of a mite predator-prey interaction model, *J. Math. Biol.*, **36** (1997), 149–168. https://doi.org/10.1007/s002850050095
14. M. C. Köhnke, I. Siekmann, H. Seno, H. Malchow, A type IV functional response with different shapes in a predator-prey model, *J. Theor. Biol.*, **505** (2020), 110419. https://doi.org/10.1016/j.jtbi.2020.110419
15. X. C. Duan, S. L. Yuan, M. Martcheva, Habitat adaption promotes the evolution of predator species, *Z. Angew. Math. Phys.*, **74** (2023), 10. https://doi.org/10.1007/s00033-022-01904-8
16. S. L. Yuan, C. Q. Xu, T. H. Zhang, Spatial dynamics in a predator-prey model with herd behavior, *Chaos*, **23** (2013), 033102. https://doi.org/10.1063/1.4812724
17. X. B. Zhang, J. Liu, G. L. Wang, Impacts of nonlocal fear effect and delay on a reaction-diffusion predator-prey model, *Int. J. Biomath.*, **18** (2025), 2350089. https://doi.org/10.1142/S1793524523500894
18. X. Chen, W. Yang, Impact of fear-induced group defense in a Monod-Haldane type prey-predator model, *J. Appl. Math. Comput.*, **70** (2024), 3331–3368. https://doi.org/10.1007/s12190-024-02101-8
19. R. L. Koch, The multicolored Asian lady beetle, *Harmonia axyridis*: A review of its biology, uses in biological control, and non-target impacts, *J. Insect Sci.*, **3** (2003), 32. https://doi.org/10.1093/jis/3.1.32

20. M. Camacho-Cervantes, A. Ortega-Iturriaga, E. del-Val, From effective biocontrol agent to successful invader: The harlequin ladybird (*Harmonia axyridis*) as an example of good ideas that could go wrong, *PeerJ*, **5** (2017), e3296. https://doi.org/10.7717/peerj.3296

21. S. Tang, L. Chen, Modelling and analysis of integrated pest management strategy, *Discrete Contin. Dyn. Syst. - Ser. B*, **4** (2004), 759–768. https://doi.org/10.3934/dcdsb.2004.4.759

22. S. Tang, R. A. Cheke, State-dependent impulsive models of integrated pest management (IPM) strategies and their dynamic consequences, *J. Math. Biol.*, **50** (2005), 257–292. https://doi.org/10.1007/s00285-004-0290-6

23. G. Jiang, Q. Lu, The dynamics of a prey-predator model with impulsive state feedback control, *Discrete Contin. Dyn. Syst. - Ser. B*, **6** (2006), 1301–1320. https://doi.org/10.3934/dcdsb.2006.6.1301

24. T. Zhang, W. Ma, X. Meng, T. Zhang, Periodic solution of a prey-predator model with nonlinear state feedback control, *Appl. Math. Comput.*, **266** (2015), 95–107. https://doi.org/10.1016/j.amc.2015.05.016

25. L. Zhao, L. Chen, Q. Zhang, The geometrical analysis of a predator-prey model with two state impulses, *Math. Biosci.*, **238** (2012), 55–64. https://doi.org/10.1016/j.mbs.2012.03.011

26. J. Wang, H. Cheng, X. Meng, B. G. S. A. Pradeep, Geometrical analysis and control optimization of a predator-prey model with multi state-dependent impulse, *Adv. Differ. Equations*, **2017** (2017), 252. https://doi.org/10.1186/s13662-017-1300-5

27. S. M. Barribeau, D. Sok, N. M. Gerardo, Aphid reproductive investment in response to mortality risks, *BMC Evol. Biol.*, **10** (2010), 251. https://doi.org/10.1186/1471-2148-10-251

28. B. W. Lee, R. E. Clark, S. Basu, D. W. Crowder, Predators affect a plant virus through density and trait-mediated indirect effects on vectors, *Food Webs*, **33** (2022), e00251. https://doi.org/10.1016/j.fooweb.2022.e00251

29. J. C. Simon, S. Stoeckel, D. Tagu, Evolutionary and functional insights into reproductive strategies of aphids, *C.R. Biol.*, **333** (2010), 488–496. https://doi.org/10.1016/j.crvi.2010.03.003

AIMS Press